

Wentai Zhang

Department of Mechanical Engineering,
Carnegie Mellon University,
Pittsburgh, PA 15213

Jonelle Z. Yu

Department of Mechanical Engineering,
Carnegie Mellon University,
Pittsburgh, PA 15213

Fangcheng Zhu

Department of Mechanical Engineering,
Carnegie Mellon University,
Pittsburgh, PA 15213

Yifang Zhu

Department of Mechanical Engineering,
Carnegie Mellon University,
Pittsburgh, PA 15213

Zhangsihao Yang

Department of Mechanical Engineering,
Carnegie Mellon University,
Pittsburgh, PA 15213

Nurcan Gecer Ulu

Department of Mechanical Engineering,
Carnegie Mellon University,
Pittsburgh, PA 15213

Batuhan Arisoy

Vision Technologies and Solutions Group,
Siemens Corporate Technology,
755 College Road,
Princeton, NJ 08540

Levent Burak Kara¹

Department of Mechanical Engineering,
Carnegie Mellon University,
Pittsburgh, PA 15213
e-mail: lkara@cmu.edu

High Degree of Freedom Hand Pose Tracking Using Limited Strain Sensing and Optical Training

The ability to track human operators' hand usage when working in production plants and factories is critically important for developing realistic digital factory simulators as well as manufacturing process control. We propose a proof-of-concept instrumented glove with only a few strain gage sensors and a microcontroller that continuously tracks and records the hand configuration during actual use. At the heart of our approach is a trainable system that can predict the fourteen joint angles in the hand using only a small set of strain sensors. First, ten strain gages are placed at various joints in the hand to optimize the sensor layout using the English letters in the American Sign Language (ASL) as a benchmark for assessment. Next, the best sensor configurations for three through ten strain gages are computed using a support vector machine (SVM) classifier. Following the layout optimization, our approach learns a mapping between the sensor readouts to the actual joint angles optically captured using a Leap Motion system. Five regression methods including linear, quadratic, and neural regression are then used to train the mapping between the strain gage data and the corresponding joint angles. The final proposed model involves four strain gages mapped to the fourteen joint angles using a two-layer feed-forward neural network (NN). [DOI: 10.1115/1.4043757]

1 Introduction

Recent advances in 3D data acquisition and tracking technologies have enabled a rapid digitization of large production plants and factories in various formats such as point clouds and triangle soups (a set of unorganized and disconnected triangles). Acquired data are utilized for the generation of digital twin of manufacturing processes, which can be used to simulate and optimize work-cell layouts while improving human operator effectiveness, safety, and ergonomics. Although the existing process simulation tools can make use of digitized factory environments in the form of point clouds, these tools still require a labor intensive manual configuring of the simulation environment such as how human workers interact with the assembly tools and how they manipulate different objects during manufacturing.

In most factory settings, human workers are usually responsible for controlling the manufacturing process by manipulating switches, buttons, and valves in automatic systems. In handcrafted lines or assembly lines, they directly operate on the workpiece or use multiple hand tools. Under both circumstances, the behaviors

of human hands are the most critical data that need to be acquired as the majority of human operations on the production line can be represented as a set of hand motions.

In this work, we address the problem of acquiring an accurate 3D model of human hand usage using a proof-of-concept instrumented glove with only a few strain gage sensors. Once available, these data can be incorporated directly into factory environment simulators, thereby alleviating the need for manual process parameter tuning. Specifically, we envision that a set of instrumented gloves will be utilized by human workers while they are performing their jobs in a real factory environment and the proposed wearable device will enable automatic data collection for understanding how human workers interact with their surroundings. The content of this paper is based on our paper [1] presented at the IDETC/CIE 2018 conference.

Toward this goal, we develop a wearable device that is able to track and record human hand poses relative to the wrist over an extended period of time. The main advance in this work is the development of methods, algorithms, and a prototype device that use as little as *four* strain gages to predict in real-time all the *fourteen* joint angles in the fingers with an average root-mean-square error (RMSE) of 3.6 deg. Given a target number of strain gages, we begin by optimizing the layout configuration of these sensors on the outer surface of the human hand using the

¹Corresponding author.

Manuscript received September 15, 2018; final manuscript received February 27, 2019; published online June 17, 2019. Assoc. Editor: Jitesh H. Panchal.

classification performance on the English letters in American Sign Language (ASL) as a way to assess candidate layouts. Next, we establish a training protocol for hand pose tracking wherein a new user wears and trains the glove for a duration of 3 min. The purpose of this training is to learn a mapping from the sensor readouts to the fourteen joint angles, where the joint angles are captured using a Leap Motion depth sensor as the ground truth. This approach enables high-fidelity benchmark poses to be gathered during the training phase using optical tracking, while alleviating the need for optical tracking during actual use (hence only requiring strain sensing). In consideration of the fabrication cost and comfort of wear, we target at using as few strain sensors as possible. The results of our experiments involving a varying number of strain gages as well as regression algorithms involving linear least squares, quadratic least squares, and neural regression are also compared. Our studies suggest that an instrumented glove with four strain gages that uses neural regression to be the best compromise between tracking accuracy and device simplicity in all the regression methods aforementioned.

Our main contributions are the following:

- (1) A method to optimize the strain sensor layout for human hand pose estimation.
- (2) A training algorithm between optically captured hand poses and a lower dimensional strain data for high fidelity hand pose tracking.
- (3) A wearable glove with a limited number of strain sensors for real-time hand pose tracking.

2 Related Work

Our work builds on hand gesture recognition and tracking systems with a specific focus on factory environment use. In this section, we review hardware systems and computational algorithms of two main hand tracking approaches: (1) wearable sensor systems and (2) vision-based techniques. Additionally, we discuss commercially available hand tracking systems in relation to our specific problem.

2.1 Wearable Sensor Systems. Wearable devices typically integrate strain, acceleration, and force sensors combined with classifiers for hand pose recognition [2–5]. Compared to these works, our aim is to track the full hand pose rather than a set of discrete hand gestures. Kramer et al. [2] present a hand gesture recognition system using an instrumented glove with approximately 20 sensors where each sensor is composed of two strain gages. In our approach, we aim to minimize the number of strain sensors for ease of usability and cost of fabrication. The musculoskeletal system of the hand allows the prediction of hand movement (all 14 joints) using fewer number of sensors due to a coupling between the joint angles. In our approach, we exploit this coupling to achieve accurate tracking using only a few sensors (3–5) with a performance similar to ten strain gages. Note that this approach requires a special attention due to the mapping from low-dimensional sensor data to a high-dimensional joint angle space (Sec. 3.3.2).

Lei et al. [4] present an accelerometer-based method to detect 12 predefined index finger movements of stroke patients during rehabilitation therapies. The study reports gesture recognition accuracy varying from 59% to 87% and continuous tracking of one finger on the 12 classes. One drawback of accelerometer-based approaches is that these sensors are rigid pieces. In contrast, strain gages are inherently slimmer, lighter, and flexible allowing them to better conform to natural hand poses. Federico et al. [3] demonstrate a glove design with conductive mixture patterns as sensors. Carbonaro et al. [6] present a wearable kinesthetic glove realized with knitted piezoresistive fabric sensor technology. Their glove is conceived to capture hand movement and gesture by using knitted piezoresistive fabric in a double-layer configuration working as angular sensors. Hammond et al. [7] demonstrate work on the design, fabrication, and experimental validation of a soft sensor-embedded glove which measures both hand motion

and contact pressures. While the above study presents very high accuracy at first wear, sensor-based approaches are sensitive to hand sizes and repetitive wears. In our approach, we overcome this issue with a short training session using a depth sensor in a controlled environment.

2.2 Vision-Based Techniques. Vision-based approaches have been widely used in gesture recognition and motion tracking applications. These vision-based approaches have been demonstrated using many different hardware setups including optical or infrared cameras [8,9], red, green, and blue (RGB) cameras, and depth sensors [10,11]. Gioliu et al. [12] present a support vector machine (SVM) based gesture recognition algorithm using infrared cameras, RGB cameras, and depth sensors, reporting up to 92% accuracy. Wang and Popović [13] use a single camera to track a hand wearing an ordinary cloth glove. da Silva et al. [14] develop a wearable sensing glove for monitoring hand gestures based on optical fiber Bragg gratings sensors. BigHand2.2M [15] uses a convolution neural network (NN) to predict the position of the joints on the input depth maps. Real-time hand tracking has been studied in Ref. [16]. However, vision-based techniques are nonwearable and nonportable settings which are not feasible in an industrial environment. Vision-based techniques are also sensitive to environment conditions such as lighting which may change during an operation in a factory. Moreover, vision-based techniques are not suitable for hand tracking while holding other objects due to occlusions.

2.3 Other Related Work and Commercial Systems. Posture recognition systems for other body parts such as the surface [5], arm [17], leg [18], and body [19,20] have also been extensively studied. Rendl et al. [5] use a transparent sensing surface based on printed piezoelectric sensors to reconstruct surfaces. Though their reconstruction of the surface can work well, it is more complicated to predict the angle of joints. In principle, these works share techniques and goals similar to that of hand tracking. Yet, the hand tracking problems require higher resolution sensor readings as well as smaller hardware restrictions for portability.

There exists a growing body of commercial hand gesture recognition and tracking systems. Proglove [21] is a wearable device that demonstrates the need for tracking operations in a factory environment. Proglove is designed to scan and display the items which are being touched or handled for industrial logistics, hence is not concerned with hand pose estimation and tracking. Gest (accelerometer-based) and Myo (acoustic-based) [22]² are wearable devices that focus on hand gesture recognition to control computers and machines. Compared to these devices, our aim is to develop a wearable system that can be incorporated into traditional work gloves with whole hand tracking capabilities. Cyber Glove [23] is a motion capture device equipped with 22 sensors for full hand tracking. In contrast, understanding redundancies and minimizing the number of sensors is key in our approach to enable development of a comfortable and affordable glove system. In addition, we introduce a training approach for personalized calibration of glove systems.

Leap Motion and Kinect [24]³ are vision-based hand tracking devices primarily for virtual reality gaming. They require external devices like cameras to be placed facing the tracked objects. Such nonportable settings requiring optical sensors are not feasible in our target context. However, these approaches are very useful for training and calibration purposes. As such, we use a Leap Motion system for the initial mapping of strain sensor data to the joint angles. By combining the strain sensor based tracking with the vision-based pretraining, we can monitor hand poses even when the hand is occluded holding an object and we can quickly train the algorithms for accurate personalized tracking. To our knowledge, our study is the first to focus on real-time hand pose tracking

²<https://gest.co>

³<https://www.leapmotion.com>

Table 1 A summary of some selected related work as a comparison to our method

Name	Approach	Adaptive to hand sizes	Adaptive to occlusions	Main focus
[2–4,21,22] ^a	Wearable	×	✓	Gesture recognition
[7]	Wearable	✓	✓	Gesture recognition
[6,23]	Wearable	×	✓	Index finger tracking
[8–12]	Vision-based	✓	×	Hand tracking
[13–16,24] ^b	Vision-based	✓	×	Gesture recognition
Our method	Wearable	✓ (trainable)	✓	Hand tracking

^a<https://gest.co>.

^b<https://www.leapmotion.com>.

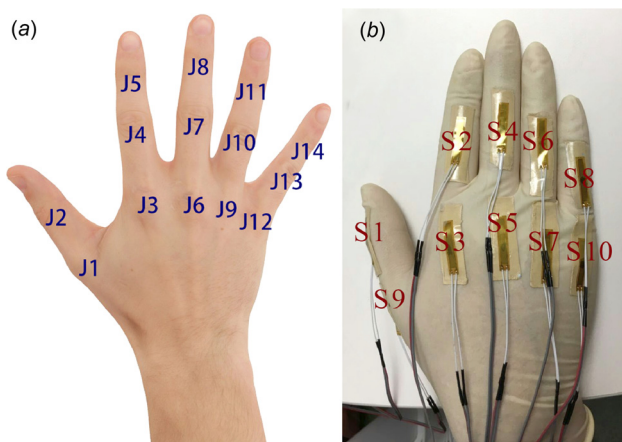


Fig. 1 (a) Fourteen joints in the hand and (b) ten strain sensor layout on a latex glove

with or without objects in hand using only a few strain sensors (see Table 1).

3 Technical Approach

In this paper, our objective is hand pose tracking using a simple and portable hardware setup and develop algorithms that address our specific challenges. We divide our technical discussions into two parts. First, we discuss the hardware design and explain our algorithms for choosing informative sensor placements. Second, we describe the hand tracking protocol and the training procedure for personalized tracking that captures the hand size and a possible initial deformation of the strain sensors.

3.1 Hardware Design and Initial Sensor Layout. As shown in Fig. 1(a), there are 14 joints in the hand. Our approach aims to track the angular deformations at these joints during the hand’s actual use. For our prototype, we choose a latex glove in order to achieve a tight fit with the hand as a way to increase strain readout fidelity. For the initial strain gage placement, we use ten strain gages as shown in Fig. 1(b). We observe that the motion of the tip joints (J5, J8, J11, and J14) are strongly coupled with the mid-joints (J4, J7, J10, and J13) at each finger making two of these joints on the same finger difficult to move independently. Based on this observation, we place only two sensors per finger, resulting in ten total sensors (S1–S10).

3.1.1 Hardware Setup. For the prototype, ten strain gages (KFH-20-120-C1-11L1M2R, Omega) are attached to a medium-sized Latex glove (Microflex[®] Diamond Grip[™], Norwalk, CT, ULINE, Pleasant Prairie, WI) using double-sided tape. The glove is worn by a human subject and the hand is laid flat on a flat surface prior to attaching the sensors as shown in Fig. 1(b). This configuration simply establishes a strain-free datum for the sensor network. Any subsequent hand motion is registered via the tensile

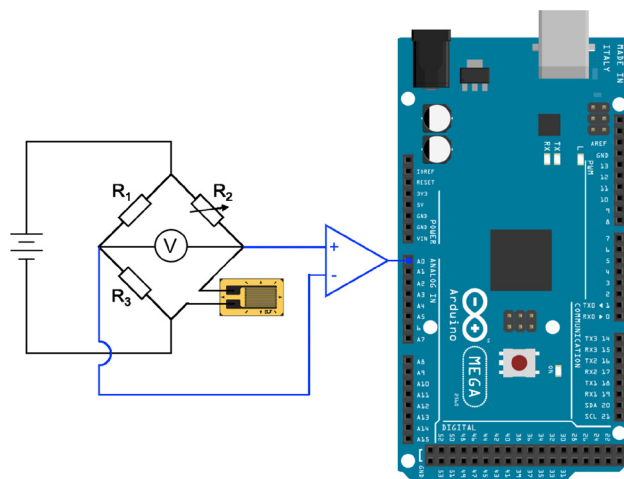


Fig. 2 The schematic design of hardware setup (1 channel)



Fig. 3 The hand gestures used in our sensor selection study. P0 corresponds to neutral hand pose that serves as a calibration point. P1–P13 are the first 13 letters (A–M) in American Sign Language. Image courtesy: Dr. Bill Vicars⁴.

or compressive strain readouts. Once the sensors are attached, this particular glove is used by all human subjects without changing the sensor locations, with user-specific training prior to the use of the glove as will be discussed in Sec. 3.3.

As shown in Fig. 2, we use an Arduino microcontroller board for the strain readouts with a Wheatstone bridge amplifier (INA125P-ND, Texas Instruments), whose output is then channeled to the analog port of the Arduino mega board to register ten strain gages.

3.2 Data Collection and Sensor Layout Optimization. In this section, we explain the data collection and sensor layout selection process to determine which sensor configurations provide the highest information gain as measured through a gesture classification system. This process is repeated for a range of target

⁴<https://www.Lifeprint.com>

Table 2 Recognition accuracy of the best five sensor configurations using three strain gages

Configuration	Training accuracy (%)	Test accuracy (%)
S5, S8, S9	98.29	63.44
S5, S6, S8	95.96	59.56
S5, S6, S9	93.11	58.72
S6, S8, S9	90.90	57.04
S7, S8, S9	94.02	50.80

sensor numbers (3–10 sensors). For each target number of sensors, we identify the best strain gage choices using the classification performance on the English letters in ASL as a way to assess the candidate sensor choices (Fig. 3). Toward this goal, three users (two males and one female) perform the static gestures for the first 13 letters of the ASL while wearing the instrumented glove. For each user, pose 0 serves as the neutral calibration point to zero all sensor readouts prior to each trial. In each iteration, the user presents pose 1 through pose 13 while holding each pose for approximately 10 s. The sensor readouts are recorded at every 100 ms. Each user repeats the experiment for the second time by taking off the glove and wearing it again. Following data collection, the transition periods between the thirteen poses (the leading and trailing two seconds for each pose) are removed.

Next, the data obtained from the three users are aggregated into a large set, separated into two bins: first time wear (all users aggregated) and second time wear (again, all users aggregated). The first time wear data are used for training, and are further broken into tenfold training and validation sets. For each target number of sensors, we use a multiclass SVM with cross validation to determine the strain gage combinations that yield the highest user-independent recognition accuracy on the ASL test.

Table 2 shows the recognition accuracy on the ASL data for sensor configurations consisting of only three sensors (top five of $C\binom{10}{3}$ choices). The training accuracy (trained on first time wear data) reports the average of the validation runs for each configuration, while the test accuracy reports the results on the test set (second time wear data). The fall-off between the training accuracy and test accuracy mainly results from the misalignment among different wearings. As shown, S5, S8, and S9 form the best three-sensor configuration.

Table 3 summarizes the best sensor choices as a function of the target number of strain gages.

3.3 Hand Tracking. After we establish the optimal sensor choices, we describe the hand tracking process. For hand tracking, the key need is to map the strain sensor readouts to the fourteen joint angles through a training protocol, and use this map as a way to predict the hand pose during actual use. However, the main challenge is in the prediction of the high degrees-of-freedom joint angles from a fewer number of sensor readouts.

3.3.1 Training for Pose Tracking: Data Collection. For training, we establish a map between the strain sensor readouts and the joint angles with the help of the Leap Motion depth sensor (Fig. 4). This system allows the capture of all fourteen joint angles in a controlled environment, thus establishing the ground truth for the strain to joint angle mapping.

During training, the users move their hands through random poses while wearing the instrumented glove. The hand motion should be slow enough for strain sensor readings to stabilize against the Leap Motion data capture. Note that this stabilization is only needed during training to match strain sensor readings to Leap Motion data. Hence, no speed restriction is present once the system is trained.

Figure 5 shows the amount of variation in each of the fourteen joint angles ($\text{abs}(\text{Angle}_{\text{max}} - \text{Angle}_{\text{min}})$) as captured through the Leap Motion system. These variations are important to note as

Table 3 Best sensor configuration for each target number of strain gages (3–9)

No. of target SGs	Best configuration
3	S5, S8, S9
4	S6, S7, S8, S9
5	S5, S6, S7, S8, S9
6	S2, S4, S5, S7, S8, S9
7	S1, S2, S4, S5, S7, S8, S9
8	S1, S2, S3, S5, S6, S7, S8, S9
9	S1, S2, S4, S5, S6, S7, S8, S9, S10

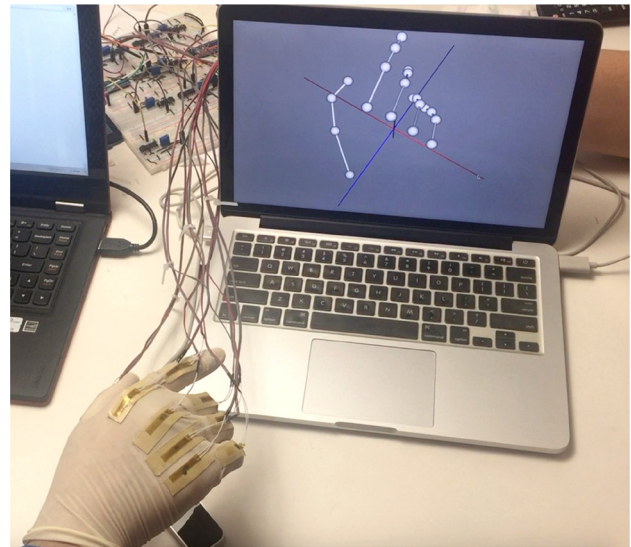


Fig. 4 Optical training process using the Leap Motion system

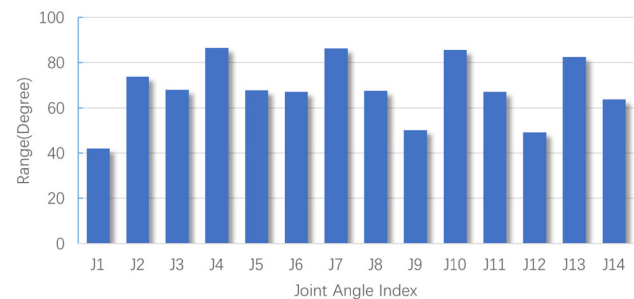


Fig. 5 The range of the joint angles captured through the Leap Motion system

they will allow an assessment of the RMSE values reported in Sec. 4.

A new user wears and trains the glove for a duration of 3 min. During this phase, the strain readouts and the joint angle readouts are captured at different frequencies, and moreover, the sampling may be nonuniform within each channel. These two input streams are thus registered by acquiring them through the same computer and using the system clock as a reference for registration. This produces a large set of registered strain versus joint angle pairs (approximately between 1500 and 1700 pairs) that are used for the next step of training. Note that this training is repeated for each new user to accommodate differences in hand shapes and sizes.

3.3.2 Training Algorithms. To map the strains to the joint angles, we use linear regression, quadratic regression, and feed-forward neural regression. Note that, for these regression models,

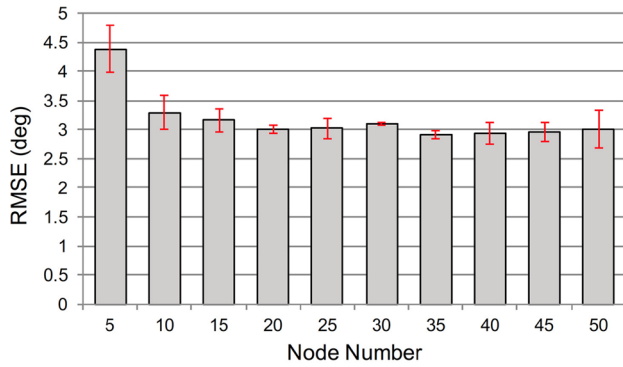


Fig. 6 RMSE for single hidden layer neural networks as a function of hidden nodes

the mapping is from k strain gages to the 14 joint angles (where $k < 14$).

Linear regression: For linear regression with bias, this map can be represented as follows:

$$S^T \mathbf{T} = J \quad (1)$$

where S is the $N \times (k + 1)$ strain data matrix (with bias), N is the number of training data points, and k is the number of target strain gages. J is the corresponding $N \times 14$ joint angle matrix encoded in a similar way. \mathbf{T} is the desired mapping matrix. We use a linear least squares solver with $L2$ regularization to obtain the map \mathbf{T} .

Quadratic regression: Quadratic regression follows a structure similar to that of the linear regression model, except the width of S and the height of \mathbf{T} are increased to account for the quadratic terms, while using the same number of training data as before.

Support vector regression: The support vector regression (SVR) uses the same principles for regression as the SVM for classification. In our case, we use the Gaussian kernel as the kernel function.

Random forest regression: Random forest regression (RFR) is an ensemble learning method for regression that operates by learning a multitude of decision trees whose predictions consolidated into a single prediction [16]. We use 100 decision trees (choice determined empirically) to learn the mapping from the strain sensors to the joint angles.

Neural regression: Finally, we build a feed-forward neural network to estimate \mathbf{T} . The network admits the strain sensor data as input and estimates the joint angle data on the output. We train various neural networks with different complexities. Both single and double layer networks are tested, with the number of hidden nodes in each layer ranging from 10, 20, ..., 50. The sigmoid activation function is used in the hidden layers. Each network is trained three times and is assessed based on the average RMSE.

4 Results and Discussion

In all of our experiments, we trained our algorithms with 90% of shuffled data and tested it with the remaining 10%.

4.1 Neural Network Optimization. We conducted parametric studies to search for a good performing neural network structure. For a single hidden layer, we varied the number of hidden nodes from 5 to 50 with an increment of five. In all cases, the training continues until an increase in the validation error is observed. The resulting average RMSE values (over different numbers of target input sensors) corresponding to a different number of hidden layer nodes are shown in Fig. 6. We deem 15 hidden layer nodes to be a good compromise between network complexity and accuracy.

Similarly, a two hidden layer network was also explored. Here, the number of hidden layer nodes in the first and second hidden layers is varied from 10 to 50 with an increment of ten. Based on

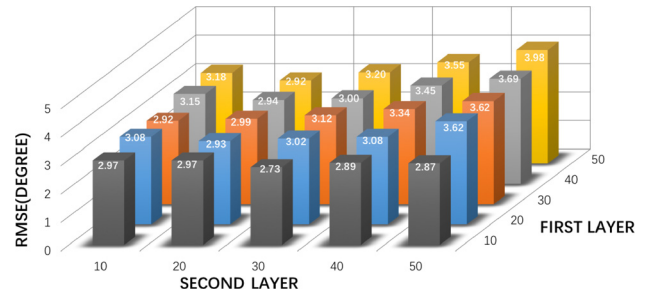


Fig. 7 RMSE for two hidden layer neural networks as a function of hidden layer nodes

the results shown in Fig. 7, we choose the network with ten first layer nodes and 30 s layer nodes (RMSE of 2.73 deg). As a comparison, the resolution and the error between wearings for Cyber Glove [23] are 1 deg and 3 deg with 22 sensors.

While the optimal single and two hidden layer networks perform well with low RMSE values relative to the joint angle ranges (Figs. 6 and 7 versus Fig. 5), we use the two hidden layer network over the single hidden layer network in the remainder of this work.

4.2 Comparison of Regression Models. Figure 8 summarizes the performance of our linear (LR), Quadratic (QR), SVR, RFR, and NN regression models, reported as the RMSE values of the models applied to the test data and averaged over the fourteen joint angles. As shown, QR, SVR, RFR, and NN produce markedly better estimations over LR (smaller RMSE is better).

For each model, as the number of sensors increases, the RMSE values exhibit a declining trend as expected. Of note is the fact that even with only four sensors, the NN produces results that are better than the ten-sensor models of LR and QR. The results of NN are slightly better than RFR and SVR model. With the number of sensors increasing, the difference between NN, RFR, and SVR models is becoming smaller. As such, we deem the NN model with four sensors as the best model to deploy with the observed data, as it provides a favorable trade-off between simplicity and test accuracy. As shown in Table 3, this result suggests the use of NN model with strain sensors S6, S7, S8, and S9.

4.3 Insights Into the Joints. Figure 9 provides a more detailed view of the RMSE values. In particular, Fig. 9 shows—for each joint—the RMSE values for the five regression models for configurations of ten sensors as well as four sensors⁵. For most joints, the NN model produces lower RMSE values. Moreover, for the proposed four-sensor configuration (Fig. 8 right), the maximum RMSE for the NN is observed at J3 and J6. Interestingly, these two joints also result in the worst RMSE values for LR and QR. And even more interestingly, these joints are also responsible for producing the worst RMSE values for the ten-sensor configuration (Fig. 8 left). On the other hand, for RFR and SVR, this observation is reversed. For the four-sensor configuration, for J3, RFR and SVR exhibit better performance over NN. Likewise, when the number of strain gages is ten, RFR and SVR perform slightly better than NN. This observation offers the insight that combining different regression algorithms using ensembles with respect to different joints may further improve the overall accuracy of our approach.

Figure 10 shows the R^2 values for the five regression models over different joints. In this case, the higher the R^2 , the better the improvement in the prediction model, compared to the mean model. As seen, the NN model is the best when it comes to explaining the variation in the data.

⁵Note that Fig. 8 reports an average RMSE over these joints.

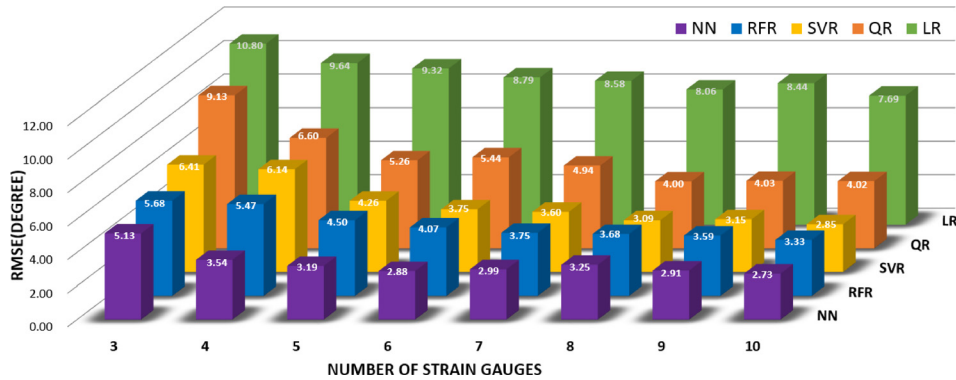


Fig. 8 Comparison between different regression models with varying numbers of target strain gages

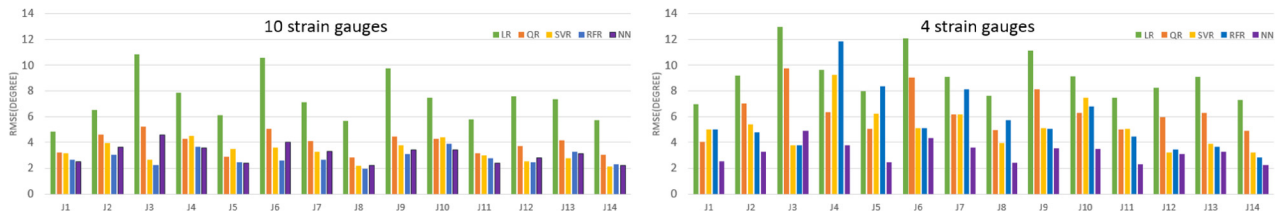


Fig. 9 RMSE of the five regression models using ten strain gauge data (left) or four strain gauge data (right)

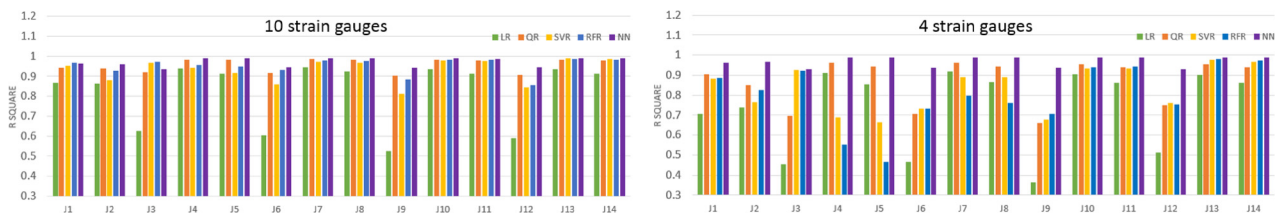


Fig. 10 R^2 of five regression models using ten strain gauge data (left) or four strain gauge data (right)

5 Conclusions

This work presents a trainable instrumented glove that is capable of predicting the fourteen joint angles on a hand using as few as four strain gages. The long-term goal of this study is to enable wearable gloves that can be used in factory settings to monitor workers' hand usage over extended periods of time. The proposed algorithms and prototype system offer a step toward this goal.

During deployment, hand pose prediction that relies solely on strain readouts has the advantage of not being restricted by bulky hardware and other impediments common to optical sensing systems such as object occlusions and lighting. Our work, however, takes a significant advantage of the optical tracking system by offering a short training phase that allows the determination of a robust mapping from the physical strain space to an optically captured joint angle space. The optical tracking is only confined to the training phase, thereby making the proposed system usable during deployment.

Our work has demonstrated that a training duration as short as 3 min provides sufficient data to learn a useful mapping from the strain gages onto the joint angles, thereby making the proposed system practically viable in real-world settings.

While our work uses conventional strain gages for the development of the methodology, the same infrastructure and algorithmic approach can be immediately adopted for use with more advanced strain sensors with smaller footprints or with those using soft materials and continuous electronic circuitry. We intend to explore this direction as the immediate next step.

5.1 Limitations and Future Work. This study is limited to the prototype glove that includes both sensing and tethered data

transmission. An immediate improvement would be to incorporate wireless data transmission. This setup would include a data receiving hardware that connects to the computer system following the same hand tracking algorithms presented in this paper.

Another future direction involves extending glove usage and data collection over durations measured in hours. This way we can investigate the performance of our hand pose tracking approach for actual use cases with long operational times.

Finally, in future studies, we intend to improve the glove ergonomics, as well as to explore using soft materials and continuous electronic circuitry in the glove to improve comfort. We envision a glove system in which both sensing and circuitry design are further informed by ergonomic considerations.

Funding Data

- Siemens Corporate Technology (Funder ID: 10.13039/501100004830).

References

- [1] Wentai, Z., Yu, J. Z., Zhu, F., Zhu, Y., Gecer Ulu, N., Arisoy, B., and Kara, L. B., 2018, "High Degree of Freedom Hand Pose Tracking Using Limited Strain Sensing and Optical Training," *ASME Paper No. DETC2018-85870*.
- [2] Kramer, J. F., George, W. R., and Lindener, P., 1994, "Strain-Sensing Goniometers, Systems and Recognition Algorithms," U.S. Patent 5,280,265.
- [3] Lorussi, F., Scilingo, E. P., Tesconi, M., Tognetti, A., and De Rossi, D., 2005, "Strain Sensing Fabric for Hand Posture and Gesture Monitoring," *IEEE Trans. Inf. Technol. Biomed.*, **9**(3), pp. 372–381.
- [4] Jing, L., Zhou, Y., Cheng, Z., and Wang, J., 2011, "A Recognition Method for One-Stroke Finger Gestures Using a MEMS 3D Accelerometer," *IEICE Trans.*, **94D**(5), pp. 1062–1072.

- [5] Rendl, C., Kim, D., Fanello, S. R., Parzer, P., Rhemann, C., Taylor, J., Zirkel, M., Scheipl, G., Rothländer, T., Haller, M. J., and Izadi, S., 2014, "FlexSense: A Transparent Self-Sensing Deformable Surface," 27th Annual ACM Symposium on User Interface Software and Technology (UIST'14), Honolulu, HI, Oct. 5–8.
- [6] Carbonaro, N., Mura, G. D., Lorusi, F., Paradiso, R., De Rossi, D., and Tognetti, A., 2014, "Exploiting Wearable Goniometer Technology for Motion Sensing Gloves," *IEEE J. Biomed. Health Inf.*, **18**(6), pp. 1788–1795.
- [7] Hammond, F. L., Mengüç, Y., and Wood, R. J., 2014, "Toward a Modular Soft Sensor-Embedded Glove for Human Hand Motion and Tactile Pressure Measurement," *IEEE/RSJ International Conference on Intelligent Robots and Systems (IROS)*, Chicago, IL, Sept. 14–18, pp. 4000–4007.
- [8] Chen, F.-S., Fu, C.-M., and Huang, C.-L., 2003, "Hand Gesture Recognition Using a Real-Time Tracking Method and Hidden Markov Models," *Image Vision Comput.*, **21**(8), pp. 745–758.
- [9] Bretzner, L., Laptiev, I., and Lindeberg, T., 2002, "Hand Gesture Recognition Using Multi-Scale Colour Features, Hierarchical Models and Particle Filtering," Fifth IEEE International Conference on Automatic Face and Gesture Recognition (*FGR 2002*), Washington, DC, May 20–21, pp. 423–428.
- [10] Ren, Z., Meng, J., Yuan, J., and Zhang, Z., 2011, "Robust Hand Gesture Recognition With Kinect Sensor," 19th ACM International Conference on Multimedia (*ACM*), Scottsdale, AZ, Nov. 28–Dec. 1, pp. 759–760.
- [11] Biswas, K. K., and Basu, S. K., 2011, "Gesture Recognition Using Microsoft Kinect[®]," Fifth International Conference on Automation, Robotics and Applications (ICARA), Wellington, New Zealand, Dec. 6–8, pp. 100–103.
- [12] Marin, G., Dominio, F., and Zanuttigh, P., 2014, "Hand Gesture Recognition With Leap Motion and Kinect Devices," *IEEE International Conference on Image Processing (ICIP)*, Paris, France, Oct. 27–30, pp. 1565–1569.
- [13] Wang, R. Y., and Popović, J., 2009, "Real-Time Hand-Tracking With a Color Glove," *ACM SIGGRAPH 2009 Papers (SIGGRAPH '09)*, New Orleans, LO, Aug. 3–7.
- [14] da Silva, A. F., Goncalves, A. F., Mendes, P. M., and Correia, J. H., 2011, "FBG Sensing Glove for Monitoring Hand Posture," *Sens. J. IEEE*, **11**(10), pp. 2442–2448.
- [15] Yuan, S., Ye, Q., Stenger, B., Jain, S., and Kim, T., 2017, "BigHand2.2M Benchmark: Hand Pose Dataset and State of the Art Analysis," *IEEE Conference on Computer Vision and Pattern Recognition (CVPR)*, Honolulu, HI, pp. 2605–2613.
- [16] Andrea, T., Matthias, S., Anastasia, T., Sofien, B., Mario, B., and Mark, P., 2015, "Robust Articulated-ICP for Real-Time Hand Tracking," *Computer Graphics Forum (Proceedings of SGP)*, **34**(5), pp. 101–114.
- [17] Zappi, P., Stiefmeier, T., Farella, E., Roggen, D., Benini, L., and Troster, G., 2007, "Activity Recognition From on-Body Sensors by Classifier Fusion: Sensor Scalability and Robustness," *Third International Conference on Intelligent Sensors, Sensor Networks and Information (ISSNIP)*, Melbourne, Australia, Dec. 3–6, pp. 281–286.
- [18] Lee, S.-W., and Mase, K., 2002, "Activity and Location Recognition Using Wearable Sensors," *IEEE Pervasive Comput.*, **1**(3), pp. 24–32.
- [19] Mattmann, C., Amft, O., Harms, H., Troster, G., and Clemens, F., 2007, "Recognizing Upper Body Postures Using Textile Strain Sensors," 11th IEEE International Symposium on Wearable Computers (*ISWC 2007*), Boston, MA, Oct. 11–13, pp. 29–36.
- [20] Kern, N., Schiele, B., and Schmidt, A., 2003, "Multi-Sensor Activity Context Detection for Wearable Computing," *European Symposium on Ambient Intelligence*, Springer, Berlin, pp. 220–232.
- [21] ProGlove, 2015, "1st Smart Glove for Industries," ProGlove, Munich, Germany, accessed Mar. 2, 2017, <http://www.proglove.de>
- [22] Myo, 2013, "Myo Gesture Control Armband," North Inc., Brooklyn, NY, accessed Mar. 2, 2017, <https://www.myo.com>
- [23] Cyber Glove Systems, 2016, "MoCap Glove System," CyberGlove Systems LLC, San Jose, CA, accessed Mar. 11, 2018, <http://www.cyberglovesystems.com>
- [24] VR Guide, 2017, "Samsung Rink: Buy VR Guide," Andreas Johannsen, Washington, DC, accessed Mar. 2, 2017, <http://www.buyvrguide.com/vr-controllers/samsung-rink/>